JOURNAL OF CATALYSIS 107, 522–534 (1987)

Reduction Behavior and Metathesis Activity of WO_3/Al_2O_3 Catalysts

I. An XPS Investigation of WO_3/Al_2O_3 Catalysts

W. GRÜNERT,* E. S. SHPIRO,† R. FELDHAUS,* K. ANDERS,* G. V. ANTOSHIN,† AND KH. M. MINACHEV†

*GDR Academy of Sciences, Central Institute of Organic Chemistry, DDR-7050 Leipzig, Permoserstrasse 15, German Democratic Republic; and †USSR Academy of Sciences, N.D. Zelinski Institute of Organic Chemistry, 117913 Moscow, Leninsky Prospekt 47, USSR

Received September 22, 1986; revised May 12, 1987

The reduction of WO_3/Al_2O_3 catalysts with 7–23 wt% WO_3 and of pure tungsten compounds was studied by XPS. In the pure compounds, W(VI) is reduced to the metal via W(V) and W(IV). An additional intermediate observed only in WO_3 may be W(II) or W(IV) engaged in a particular interaction. In the reduction of $Al_2(WO_4)_3$ a stabilization of W(VI) and W(IV) relative to Al-free samples is observed at high reduction temperatures. On the Al_2O_3 support the reduction of W(VI) starts at substantially higher temperatures than that in pure compounds. The stabilization is highest at low WO_3 content, where the severe conditions required for W(VI) reduction lead to the direct formation of metallic W. At WO_3 loadings near the theoretical monolayer capacity of the Al_2O_3 support, the lower temperatures of reduction permit the detection of W(IV) as an intermediate. Metallic W on Al_2O_3 exhibits a negative XPS shift relative to the bulk metal.

INTRODUCTION

Tungsten oxide and molybdena-based catalyst systems have received much attention in recent catalytic research because of their high metathesis activity and the instructive parallelism between the homogeneous and the heterogeneous catalyst versions (*1*). The discussion of the reaction mechanism of the heterogeneous metathesis has been effectively stimulated by the homogeneous analogon which yielded strong evidence for a route involving metal (oxo) alkylidene complexes (*2, 3*). On the other hand, heterogeneous systems well suited for modern surface analytic techniques may serve as models in the investigation of the catalytically active sites.

Unfortunately, evidence is not yet unambiguous in the latter field. Most authors ascribe the catalytic activity to reduced species (*4, 5*) (Me^{5+} (*6*), Me^{5+} pairs (*7*), Me^{4+} (*8–10*), with Me = W, Mo), while Me^{6+} has been considered merely a coordination center (*8*) or an active site precursor inferior to Me^{4+} (on MoO_3/Al_2O_3 (*11*)). Further elucidation of this problem may be expected from the WO_3/Al_2O_3 system, which is known to be highly resistant to reduction (*12, 13*) and is yet an active catalyst for propene metathesis (*5, 14*).

In this series, some results concerning reduction and metathesis activity of WO_3/Al_2O_3 catalysts will be reported beginning with an XPS investigation of this system. In the future, an ESR study of WO_3/Al_2O_3 catalysts and an investigation of their behavior in the metathesis of propene will be presented.

The extraordinary stability of W(VI) on Al_2O_3 has been ascribed in the literature to interactions between the alumina surface and the tungsten species, which are spread on the surface as a monomolecular layer. The interaction strength depends on the tungsten content decreasing with increasing tungsten loading. Beyond monolayer coverage, the buildup of a bulk WO_3 phase was

0021-9517/87 $3.00

observed (*12*). Hence, in an XPS investigation, the reduction of W(VI) to metallic W at 823 K was found to proceed on catalysts with WO_3 loading exceeding the theoretical monolayer coverage (*12*) while no reduction could be detected on catalysts with lower WO_3 loading at this temperature (12, 15, 16). According to (*17, 18*) the tungsten surface phase remains segregated when the pore system of the alumina is destroyed by thermal treatment at 1070–1320 K. Hence, WO_3 and, at higher calcination temperatures, $Al_2(WO_4)_3$ may be obtained starting from surfaces that contain less than a monolayer of tungstate species at moderate calcination temperatures (820 K).

The structure of the W(VI) surface complexes in submonolayer catalysts has been discussed controversially on the basis of essentially identical Raman spectra, with tetrahedral (*12*) or bridged distorted octahedral (*15*) tungstate species assumed to interact with the Al_2O_3 surface. Evidence for an octahedral WO_3-like phase which is formed at higher WO_3 loadings (*12*) has been reinterpreted with regard to Raman cross sections as indicative of a very low fraction (<4% of total W) of bulk WO_3 (*19*). This would support the view of (*20*) that tetrahedral tungstate species prevail up to high WO_3 loadings. Recently, Soled *et al.* (*21*) have observed by XPS the formation of metallic W during the severe reduction (1073–1173 K) of a submonolayer catalyst. In our study, which includes some pure tungsten compounds as well, similar reduction temperatures (823–1123 K) were applied to catalysts of different (submonolayer) WO_3 loadings. The results reveal additional spectral features of these systems and yield complementary evidence on the reduction of submonolayer WO_3/Al_2O_3 catalysts relevant to their catalytic properties.

EXPERIMENTAL

Materials. WO_3, analytical grade, and $Al_2(WO_4)_3$ were supplied by Reachim, Moscow, and Chemapol, Prague, respectively. WO_3 was calcined in air at 823 K for 2 h prior to use.

The catalyst samples were prepared by impregnation of γ-Al_2O_3 (VEB Leuna-Werke, Leuna, GDR) with a solution of WO_3 in NH_4OH by the incipient wetness technique (pH of the impregnation solution, 8.8). After impregnation, the catalysts were dried at 400 K and calcined in air at 823 K for 2 h. Nominal and actual WO_3 contents and BET areas after calcination are presented in Table 1, where the code used to denote the samples is also explained.

H_2 and Ar from cylinders were deoxygenated over MnO/Al_2O_3 and dried over $Mg(ClO_4)_2$.

Apparatus and procedure. An AEI ES 200B spectrometer (Al$K\alpha$ excitation if not stated otherwise, FRR analyzer mode) was

TABLE 1

WO_3 Contents and BET Areas of the Catalysts

Code	WO_3 content. (wt.%)		BET area		BET area after 2 h air calcination	
	Nominal	Real[a]	(m^2/g)	(m^2/g Al_2O_3)	T_{calc} (K)	Area (m^2/g)
W7	7.00	6.80	248	262	1093	189
W12	11.60	11.30	235	165	—	—
W23	23.20	23.30	203	265	973	197

[a] Determined by electron microprobe analysis.

used for this investigation. Sample pretreatment was performed outside the spectrometer in a pretreatment reactor supplied with a sample transfer lock, which is described in detail elsewhere (*22*). In a typical experiment, samples pressed into loops of nickel wire and mounted on a special sample probe were inserted into the pretreatment reactor, heated in Ar (6 liters/h) to the reduction temperature chosen, and reduced in H_2 (6 liters/h at atmospheric pressure) for 2 h. After reduction the samples were cooled in Ar, the pretreatment reactor unit was attached to the spectrometer, and the sample was transferred to the fast insertion lock of the spectrometer in an Ar protective gas atmosphere.

The spectra were accumulated, smoothed, and integrated with a Nicolet MCA. Unresolved lines (mainly W 4*f* signals) were transferred unsmoothed to the PDP 11/O3L computer incorporated in an XSAM 800 spectrometer of Kratos Ltd.

The unresolved W 4*f* spectra were subjected to a nine-point least-squares quadratic smoothing and were fitted with a standard peak synthesis program, in which spectra are composed of arbitrary Gaussian singlet lines. Constraints suited to constitute the spin doublet character of the line pairs, e.g., ratios of linewidths and intensities, binding energy splitting, had to be imposed by the user.

Quantitative analysis was complicated by additional spectral features in the case of W(VI) and W(0). A small peak with a binding energy (B.E.) ~6 eV higher than W $4f_{7/2}$ was observed for all W(VI) compounds (Figs. 1a and 1f; see also (*22*)). It exhibited a complex behavior on reduction (relative intensity enhanced in WO_3, diminished in $Al_2(WO_4)_3$ and WO_3/Al_2O_3 catalysts, see Figs. 1 and 3), which may not be unaffected by baseline effects. Moreover, according to standard B.E. tables, the W $5p_{3/2}$ peak would be expected at a B.E. approximately 3 eV higher than W $4f_{7/2}$, i.e., superimposed on W $4f_{5/2}$, with a Scofield cross section ~8% that of the total W 4*f* signal (*23*).

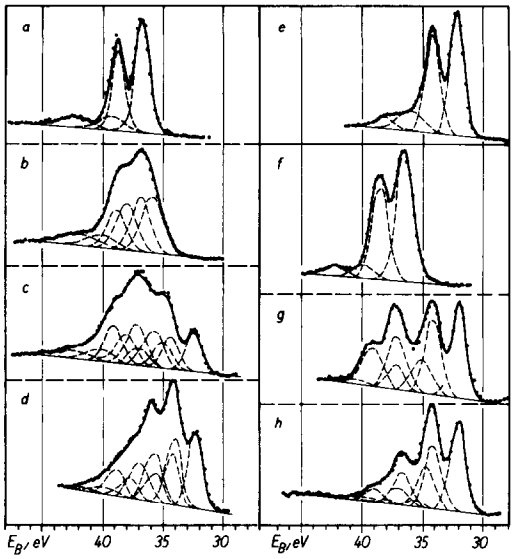

FIG. 1. W 4*f* spectra of individual tungsten compounds WO_3 after 2 h calcination in air at 823 K (a), after 2 h reduction in H_2 at 673 K (b), 823 K (c), 923 K (d), 973 K (e) (bulk W metal). $Al_2(WO_4)_3$ "as received" (f), after 2 h reduction in H_2 at 923 K (g), 973 K (h).

Considering the high energy peak mentioned above as one of a pair of satellites separated by 4.0–4.2 eV from the corresponding W 4*f* components we succeeded in analyzing the spectra of the pure W(VI) compounds by applying the Scofield intensity ratio of 0.78 (*23*) to the components of both the main line and the satellite pair. Hence, we conclude that the contribution of W $5p_{3/2}$ to the form of the signal envelope should be small, possibly due to a high peak width. The W $4f_{5/2}$: W $4f_{7/2}$ intensity ratio of 0.78 (±0.03) and a B.E. splitting of 2.1 (±0.1) eV were adopted for all tungsten oxidation states. Due to the general line broadening in the case of supported W(VI) the satellite pair was represented by a single broad peak in these spectra. A small high energy shoulder observed in the spectrum of W(0) (see following section, Fig. 1e) was neglected in the curve fitting. Possible inaccuracies due to these simplifications should not affect the essential conclusions of our work.

Binding energies were determined with an accuracy of 0.2 eV and referred to C 1*s* = 285.0 eV. However, in the case of the WO_3/Al_2O_3 catalysts, this calibration tended to yield a shift on the order of 0.5–1 eV for all lines after reduction at 973 K and above. Obviously, the C 1*s* calibration may become inadequate when samples are subjected to severe reduction procedures. In our case, the W 4*f* lines were referred to Al 2*p* = 75.1 eV and O 1*s* = 531.4 eV, the mean values obtained with the C 1*s* calibration for a large number of oxidized or mildly reduced Al_2O_3-based samples. In Table 4, W 4*f* data referred to Al 2*p* are given with values referred to O 1*s* added in parentheses if the deviation is larger than 0.1 eV.

RESULTS AND DISCUSSION

Pure Compounds

Stoichiometric substances. In Table 2, B.E. and intensity ratios of the main peaks are listed for WO_3, W metal, and $Al_2(WO_4)_3$, and compared with literature data. The W 4*f* spectra are shown in Fig. 1 ((a) WO_3, (e) W, (f) $Al_2(WO_4)_3$). W metal was obtained by severe reduction of WO_3 (2 h, 973 K) and was pyrophoric when removed from the spectrometer. The high energy shoulder of the W 4*f* signal, which has already been mentioned in the experimental section, is most probably due to spectral features of the zero valent state (contributions of W $5p_{3/2}$, possibly of plasmon excitation) though it may be repre-

TABLE 2

Binding Energies (eV) and Relative Intensities of Elements in Nonreduced Pure Compounds; Comparison with the Literature

(a) WO_3, W metal

Binding energy W $4f_{7/2}$			O 1*s*	Atomic ratio[a] W : O	Ref.
W(VI)	W(0)	ΔE_B			
36.0	31.8	4.2			*16*
36.3[b]	31.7[b]	4.6			*27*
35.7	31.4	4.3			*26*
35.9[b]	31.7[b]	4.2	530.7[b]		*12*
35.4[b]	31.1[b]	4.3	531.4[b]	1 : 3.3	*25*
36.6	32.4	4.2	530.1	1 : 3.0	This work

(b) $Al_2(WO_4)_3$

Binding energy			Atomic ratio[a] Al : W : O	Ref.
W $4f_{7/2}$	Al 2*p*	O 1*s*		
36.5 (36.2)[c]				*16*
36.5[b]	74.9[b]	531.5[b]		*12*
35.8[b]	74.5[b]	532.2[b]	8.2 : 1 : 19.3	*25*
36.7	75.2	531.0	1.1 : 1 : 5.6	This work

Note. O 1*s* = 285.0 eV or Au $4f_{7/2}$ = 84.2 eV (*12*).

[a] From intensity ratios using $\left(\frac{n_1}{n_2}\right) = \frac{I_1 \cdot \sigma_2}{I_2 \cdot \sigma_1}\left(\frac{E_{k2}}{E_{k1}}\right)^{3/2}$ (*28*); σ values from (*23*).

[b] Originally referred to Au 4*f*.

[c] ( ), calcined at 1173 K.

sented by two lines in the B.E. range of W(V)/W(VI). It was not affected by a 1-h Ar ion bombardment, which diminished the O 1*s* and C 1*s* intensities by 40–50%, and is present in literature spectra as well (*24*). The handling of pyrophoric tungsten without reoxidation in the transfer equipment suggests that reoxidation should be of minor importance with the remaining samples as well (see also (*22*)).

Table 2 reveals that our W $4f_{7/2}$ B.E. for WO_3 and W are 0.6–0.7 eV higher than the average of the literature data, while our O 1*s* value seems to be low. Such discrepancies, which are often met when B.E. data measured on different instruments are compared, may be explained by divergent procedures in energy scale calibration. The chemical shifts (ΔE_B) reported are not affected by this, as is demonstrated by the good coincidence for ΔE_B of W 4*f* between WO_3 and W, but also of O 1*s* between WO_3 and $Al_2(WO_4(_3$ when our results are compared with the literature data.

Bearing this is mind, no significant B.E. difference between the W(VI) species in WO_3 and $Al_2(WO_4)_3$ (and $(NH_4)_{10}W_{12}O_{41}$ as well (*22*) can be established by our data. The W 4*f* linewidth (FWHM) is somewhat larger in aluminium tungstate (1.8–1.9 eV) than in WO_3 and in ammonium paratungstate (*22*) (1.5–1.6 eV). The intensity ratios for the main lines correspond closely to those reported in (*25*) for WO_3 while significant deviations are noted for $Al_2(WO_4)_3$ where the W 4*f* intensity in (*25*) appears to be low.

Partially reduced samples. W 4*f* spectra illustrating the reduction of WO_3 and $Al_2(WO_4)_3$ are shown in Fig. 1. The tungsten states occurring in the reduction process are characterized in Table 3 (W $4f_{7/2}$ B.E., percentage of total W 4*f* signal area). A linear relation between the B.E. of the species and their assumed oxidation number has been found in the literature for the reduction of WO_3 (*21, 26, 27*). Figure 2 shows that this relationship holds for the reduction of $Al_2(WO_4)_3$ and $(NH_4)_{10}W_{12}O_{41}$

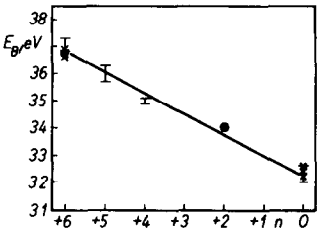

FIG. 2. Relationship between W $4f_{7/2}$ binding energies and oxidation numbers (*n*) of tungsten states (including ammonium paratungstate (*22*). (x) Data of individual compounds, (I) range found in partially reduced samples, (●) "W(II)" state in partially reduced WO_3.

as well and suggests that the tungsten states should be assigned to W(VI), W(V), W(IV), and W(II), and W(0). However, the fact that "W(II)" is observed only in the reduction of WO_3 implies that its occurrence may correspond to a structural feature typical of this compound, supporting the view of Haber *et al.* (*27*) who assigned the "W(II)" signal to W(IV) ions paired in edge sharing octahedra on shear planes.

In Table 3, it can be seen that the W(VI) B.E. tends to increase on reduction, i.e., when several oxidation states coexist, while W(0) remains in the range of 32.2 ± 0.2 eV. This tendency, which has also been found in the case of ammonium paratungstate (*22*), is reflected in the B.E. difference between W(VI) and W(0), which changes from 4.2–4.4 for individual substances to 4.6–5.0 for coexisting states. The uncertainties of the curve-fitting procedure may cast some doubt upon the significance of these shifts. However, in the course of the reduction of $Al_2(WO_4)_3$ we obtained spectra where a W(VI)/W(0) B.E. difference of ~5 eV can be clearly observed because of the predominance of these states (Fig. 1g). A similar increase in the B.E. on partial reduction has been found recently for Zr3d of Zr^{4+} in intermetallic hydrides ($ZrCr_2H_{3.6}$ (*29*), $ZrMo_2H_{1.9}$, $ZrW_2H_{1.8}$ (*30*)).

The origin of the phenomenon is not yet clear. Differential charging cannot be ruled

TABLE 3

Binding Energies (eV), Relative Intensities of Tungsten States, and Intensity Ratios of Main Lines in the Reduction of WO_3 and $Al_2(WO_4)_3$

Sample	Reduction temperature (K)	Intensity ratio			O 1*s*	Binding energy W $4f_{7/2}$(% of W 4*f* signal)			
						I (W(VI))	II	III [III*]	IV (W(0))
		W 4*f*: O 1*s*							
WO_3									
	(Nonreduced)		2.2		530.1	36.6 (100)	—	—	—
	673		2.3		530.8	36.8 (54)	35.8 (46)	—	—
	823		3.4		530.9	37.1 (37)	35.7 (23)	34.9 (17)	32.2 (21)
	923		4.8		531.0	36.8 (26)	35.8 (14)	[34.0 (30)]	32.2 (30)
	973		11, 13[b]		530.5–7	—	—	—	32.4 (100)[a]
		W 4*f*: O 1*s*	W 4*f*: Al 2*p*	Al 2*p*: O 1*s*					
$Al_2(WO_4)_3$									
	(Nonreduced)	1.2	19.6	0.064	531.0	36.7 (100)	—	—	—
	673[d]	1.5	16.7	0.087	531.3	36.9 (66)	35.9 (34)	—	—
	823[d]	2.0	11.3	0.18	531.1	37.2 (37)	36.2 (22)	34.9(24)	32.5 (17)
	923	1.2	8.0	0.14	531.6	37.1 (32)	—	35.1 (20)	32.0 (48)
	973	1.2	7.1	0.18	531.2	37.1 (12)	36.0 (5)	34.8 (29)	32.2 (54)

[a] 32.4 ± 0.2 eV, average of two samples obtained by reduction of WO_3 and a third originating from ammonium paratungstate (all W 4*f* spectra indistinguishable).

[b] O 1*s* and C 1*s* intensities comparable.

[c] Al 2*p* = 74.9–75.3 for all runs.

[d] Mg$K\alpha$ excitation, intensities corrected according to (23).

out though W metal is not present in all samples concerned. The B.E. increase may also be due to modified electronic interactions between tungsten species and between tungsten and oxygen in the defect structures of the partially reduced samples, which may also be reflected in the considerable shift of O 1*s* in the reduction of WO_3 (Table 3). Interactions between tungsten and aluminum may be superimposed in the case of $Al_2(WO_4)_3$.

In the literature, the reduction of WO_3 has been reported to be complete at 823 K (*13, 16*). We found, in accordance with (*31*), that the WO_3 reduction proceeds in a large temperature range. Major differences between the reduction behaviors of WO_3 and $Al_2(WO_4)_3$ are found in the 923- to 973-K region. While the reduction of WO_3 is complete at 973 K W(VI) and W(IV) are left in considerable amounts in the reduction of $Al_2(WO_4)_3$ under these conditions. Obviously, there is a stabilization of high valence W ions in $Al_2(WO_4)_3$, which may be similar to the well-known stabilization of W(VI) on the Al_2O_3 support ((*12, 13*), cf. section entitled "WO_3/Al_2O_3 Catalysts") as Al^{3+} ions are present in this sample. The relatively easy onset of the $Al_2(WO_4)_3$ reduction implies that the original structure does not permit such an interaction and must be reconstructed.

X-ray diffraction of $Al_2(WO_4)_3$ reduced at 923 K (transfer in contact with air) failed to detect Al_2O_3 as well as $Al_2(WO_4)_3$ and other compounds. Only metallic tungsten was identified. Nevertheless, we assume that amorphous structures of Al^{3+} and O^{2-} ions are formed, which are capable of interacting with W(VI) and W(IV) in a way similar to Al_2O_3. The O 1*s* B.E. lies in the interval of 531.1–531.6 eV for all reduction temperatures. In Al_2O_3, O 1*s* is typically found at 531.4 eV.

The W 4*f*/O 1*s* intensity ratio of WO_3 grows with increasing reduction temperature due to the progressive removal of oxygen (Table 3). In the case of the $Al_2(WO_4)_3$, the situation is more complex. In the low temperature region, W 4*f*/O 1*s* and Al 2*p*/O 1*s* increase due to the removal of oxygen while the decreasing W 4*f*/Al 2*p* ratio may indicate the beginning structural rearrangement mentioned above. The significant decrease in the W 4*f*/O 1*s* ratio at 923 K may arise from an agglomeration of the tungsten metal, which is detectable by XRD even after exposure to air.

WO_3/Al_2O_3 Catalysts

W(VI). In Table 4, the W $4f_{7/2}$ binding energies of tungsten states and their percentages of the total signal area are summarized for the reduction of the WO_3/Al_2O_3 catalysts. The absolute B.E. values may contain an instrumental shift of +0.6–0.7 eV (see section entitled "Stoichiometric Substances").

The main signal in these spectra can be represented by a doublet with a B.E. close to that of W(VI) in compounds of hexavalent tungsten but with increased linewidth (2.3–2.5 eV compared to 1.5–1.9 eV). Such line broadening is often met in XPS of supported material and has been attributed to inhomogeneous surface charging or to nonuniform interactions of the corresponding species with the support (*28*).

An increase in the Al 2*p* and the W 4*f* FWHM with decreasing WO_3 content, which may serve to identify surface charging effects in WO_3/Al_2O_3 (*12*), was detected with our samples only after thermal treatment in Ar (973 K, 1 h). In the oxidized samples, linewidths were practically constant while a significant decrease was observed after thermal treatment in H_2 even when reduction was not effected (0.4–0.6 eV for O 1*s*, 0.1–0.3 eV for Al 2*p*). These changes may be ascribed to the removal of surface oxygen (OH, O_{ads}) from the sample.

Signal shapes similar to those shown in Figs. 3a and 3b may also arise from the superposition of different valence states (W(VI) and W(V), see Fig. 1b). However, no support for the existence of W(V) already in the oxidized samples was found in

TABLE 4

W $4f_{7/2}$ Binding Energies (eV) and Percentages of Total W $4f$ Signal Area of Tungsten States Occurring in the Reduction of WO_3/Al_2O_3 Catalysts

Weight percent WO_3	Reduction temperature (K)	Binding energy			C 1*s*	W(0) content area(%)
		W(VI)	W(0)	ΔE_B		
7	—	36.3	—	—	285.1	—
	823	36.4	—	—	284.8	0
	973	37.2 (36.7)	—	—	284.8	0
	1023	36.7	—	—	285.0	285.0
	1073	36.5	31.3	5.2	284.7	12
11.6	—	36.4	—	—	284.8	—
	823	36.5	—	—	284.7	0
	973	36.6	31.4	5.2	284.2	5
	1023	36.6	31.1	5.5	284.3	5
	1073	36.6	31.1	5.5	284.5	16
	1093	36.4	31.6	4.8	284.7	41
23.2	—	36.6 (36.8)	—	—	284.8	—
	823	36.4	—	—	284.3	0
	973	36.6	31.6	5.0	284.0	10[a]
	1023	36.7	31.5	5.2	284.2	25
	1073	36.6	31.4	5.2	284.8	47
	1093	36.4	31.6	4.8	284.6	61

Note. Al $2p$ = 75.1 eV; ( ), O 1*s* = 531.4 eV.
[a] Plus 10% W(IV), E_B = 34.8 eV.

our ESR study (*32*). Moreover, the invariability of the signal shape over a wide range of reduction conditions (Figs. 3b–3e) implies that the signal arises from a single state, W(VI), the line broadening being due to nonuniform interactions with the support.

The extraordinary stability of W(VI) on Al_2O_3 is confirmed by our results: Its reduction starts at substantially higher temperatures than that of the pure tungsten compounds. The analogy of the stabilization of W(VI) on Al_2O_3 and in $Al_2(WO_4)_3$ under severe but not under mild conditions has been mentioned above. The reducibility of the WO_3/Al_2O_3 catalysts increases with growing WO_3 content, most probably due to the nonuniformity of the interactions between the tungstate species and the support. On the W23 sample reduction proceeds at 973 K while no reduction was observed with W7 even at 1023 K (Table 4). (The latter statement neglects a small concentration of W(V) that was detected by ESR (*32*) in quantities far below the detection limits in XPS spectra of this kind, which amount to ~2% of the total W for W(0), 4–5% for W(IV), and 12–15% for W(V)).

An attempt to accelerate WO_3/Al_2O_3 reduction by the spillover of activated hydrogen by analogy with the experiment of Benson *et al.* (*33*) was not successful. After treatment of a 1 : 1 physical mixture of W23 with a 2 wt% Pt/Al_2O_3 catalyst with H_2 at 823 K no reduction of W(VI) could be detected, the W $4f$ signal being completely identical to that shown in Fig. 3b.

W(0). In almost all experiments, W(0) was the only reduction product observed (Table 4). Its B.E. (31.1–31.6 eV) is shifted by −0.8–−1.3 eV relative to the pure W metal. This is reflected by an increase in ΔE_B between W(VI) and W(0), which in

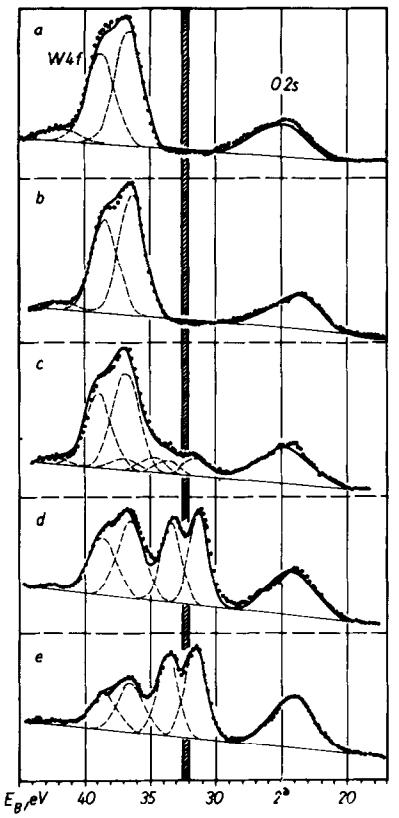

FIG. 3. W 4*f* spectra of W23 after different reduction procedures; unreduced, 2 h calcined in air at 823 K (a), 2 h reduced in H_2 at 823 K (b), 973 K (c), 1073 K (d), 1093 K (e). The shaded region indicates the B.E. range found for bulk W metal.

nearly all cases markedly exceeded the values obtained for pure substances and for W(VI) and W(0) coexisting in partially reduced samples (Tables 2 and 3).

XPS line shifts between supported and bulk metals have been extensively studied in recent years inspired by the interest in the SMSI effect. Positive shifts, which are due to final state effects, are found in many cases (*28, 34, 35*). Negative shifts due to a SMSI have been recently observed in the Rh/TiO_2 system (*36*). In a previous paper, we reported a remarkable negative shift for chromium on Al_2O_3 (−1.5 to −2.0 eV) and ascribed it tentatively to an interaction of Cr(0) with reduced spots of the support (*37*). We found a similar behavior for $Mo(O)/Al_2O_3$ (*38*). The origin of these negative shifts of Group VI metals on Al_2O_3 is not clearly established. A contribution of differential charging cannot be entirely ruled out at present though no anomaly was detected with other lines of the spectra and the absence of an analogous effect in other Me/Al_2O_3 systems would need further explanation.

The FWHM of our W(0) lines was 1.8–2.0 eV in all cases in contrast to the broad signals found by Soled *et al.* at high reduction degrees (*21*). This broadening may be due to the sample preparation technique applied (catalyst powder pressed into conducting material), which might encourage inhomogeneous charging of the W metal. The narrowing of the W 4*f* signal when one proceeds from W(VI) to W(0), which was observed in our study, suggests that the interaction between Al_2O_3 and tungsten specific to its hexavalent form is destroyed in the reduction process.

W(IV). The attention paid in the literature to W ions of intermediate valency as possible active sites of the metathesis reaction raises the question of whether such ions are present in the reduced WO_3/Al_2O_3 samples. Until now, intermediate W oxidation states have not been detected by ESCA in the reduction of WO_3/Al_2O_3 catalysts (*12, 21*). This observation is confirmed by our study for the catalysts W7 and W12 where H_2 treatment brings about a decrease in the linewidth of the W(VI) signal (compared to oxidized as well as to Ar-treated samples) rather than an increase that might indicate the presence of reduced W ions.

In the case of W23, however, a 2-h reduction at 973 K produced a W 4*f* spectrum that could not be analyzed consistently without including a contribution of an intermediate W form, which would be W(IV) according to its B.E. (Fig. 3c, Table 4). The situation is displayed in more detail in Fig. 4 where W 4*f* spectra obtained with this catalyst under different reduction conditions are compared with the signal of an Ar-treated sample (curve 1; the experimen-

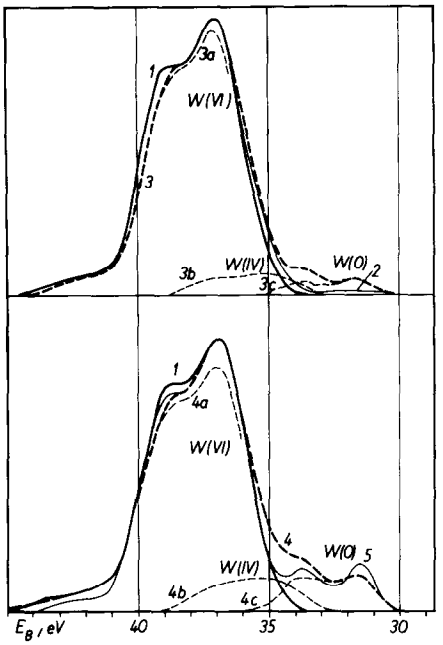

FIG. 4. Identification of W(IV) in W 4*f* spectra of W23. Sample treatments: curve 1, 40 min Ar, 973 K; curve 2, 30 min H_2, 973 K; curve 3, 70 min H_2, 973 K; curve 4, 120 min H_2, 973 K; curve 5, 10 min H_2, 1123 K. Curves 3a, 3b, 3c (4a, 4b, 4c)—W(VI), W(IV), and W(0) components of curve 3 (4).

tal points are omitted for the sake of clarity). While a 30 min reduction at 973 K causes only a slight broadening of the W 4*f* signal (curve 2) continued reduction at this temperature produces spectra (curves 3 and 4, the latter corresponding to Fig. 3c), the course of which in the 33- to 36-eV region cannot be fitted by a mere superposition of the W(0) and W(VI) components (3c, 4c, and 3a, 4a, resp., curve 1 providing an upper limit for the W(VI) component). Spectrum 5 originates from a W23 sample, in which an analogous reduction extent had been obtained under more severe conditions (1123 K, 10 min). A comparison of spectrum 5 with spectrum 4 shows directly, without reliance to curve fitting, that the intermediate is not present in spectrum 5 and supports the identification of W(IV) in spectra 3 and 4.

Certainly, the broadening of the W(VI) signal observed after 30-min reduction at 973 K (curve 2) and, analogously, after 2 h at 923 K, may also be ascribed to a contribution of W(IV). After 2 h reduction at 1023 K a W(IV) signal could no longer be identified. In a further part of this series it will be shown that the formation of an intermediate W species under the reduction conditions employed here is reflected in the catalytic behavior of W23 in the metathesis of propene.

W(IV) may have been formed also in WO_3/Al_2O_3 catalysts, which were subjected to prolonged reduction at 823 K (*12*), with the WO_3 content exceeding the monolayer capacity. An analysis of W 4*f* signal shapes from (*12*) according to the principles applied in this work required contributions of 8–14% rel. of W(IV) for the corresponding samples.

Monolayer character of WO_3/Al_2O_3 catalysts. In (*12*) it was verified that the XPS spectra of WO_3/Al_2O_3 catalysts exhibit proportionally between the W 4*f*/Al 2*p* intensity ratios and the corresponding bulk atomic ratios as long as the monolayer coverage is not arrived at. This proportionality was reproduced by us for oxidized and mildly reduced catalysts (Fig. 5). It did not hold, however, for extensively reduced samples. While the decrease in the W 4*f*/Al

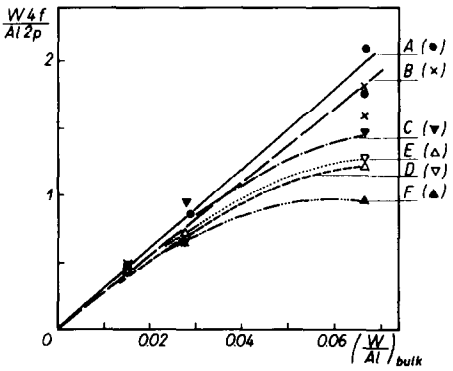

FIG. 5. Variation of the W 4*f*/Al 2*p* intensity ratio as a function of the bulk atomic W/Al ratio. Samples unreduced (A), 2 h reduced in H_2 at 823 K (B), 973 K (C), 1023 K (D), 1073 K (E), 1093 K (F).

2*p* ratio on severe reduction is within the limits of experimental error for W12 it is significant for W23. The decrease in the relative W signal intensity may be due to an agglomeration of the W metal formed.

The occurrence of tetravalent tungsten in a catalyst of high WO_3 loading (~70% of monolayer coverage) raises the question of whether W(IV) may be derived not from the surface tungstate monolayer but from a segregated WO_3 phase. In catalysts with WO_3 loadings exceeding the monolayer capacity the segregation of WO_3 has been proved by Raman spectroscopy and any reduced tungsten forms obtained with such catalysts at temperatures as low as 823 K (*12*) may be ascribed to this phase. The segregation of WO_3 might well begin when the monolayer coverage of the Al_2O_3 surface has not yet been attained, and small quantities of WO_3 crystallites would not be detected by the relatively coarse intensity correlation demonstrated in Fig. 5.

However, the quantity of crystalline WO_3 in a catalyst with a WO_3 loading comparable with our W23 sample has been shown by Raman spectroscopy to be very small (~1 wt% (*19*)). An additional segregation of WO_3 due to our thermal treatments can be excluded as the pore system of the support is practically stable at the temperatures applied (see BET data in Table 1). Unfortunately, Raman data proving the phase composition of the tungsten in our samples, which have been prepared using rather straightforward methods, are not available. However, from the general reduction behavior observed with these samples it can be concluded that they are not essentially different from those described in the literature (*5, 12, 21*). Moreover, our data show that W(IV) is not stable in WO_3 at a reduction temperature of 973 K where it is observed in W23 and in $Al_2(WO_4)_3$. Hence, W(IV) is stabilized by the alumina, and if it is derived from WO_3 crystallites it should be located at the interface with the support.

We prefer another view that takes into account the inhomogeneity of the interactions between the surface tungstate species and the support and underlines the analogies to the MoO_3/Al_2O_3 system. At low WO_3 loadings, hexavalent tungsten is stabilized by the alumina to such a degree that its reduction requires conditions where other tungsten states are not stable. The strength of the interaction (and, likewise, the reduction temperature) decreases with increasing tungsten content already at loadings far below the monolayer coverage, probably due to varying properties of the surface sites occupied by the tungstate entities or, at higher coverages, due to interactions within the tungstate layer. Thus, near monolayer coverage, the temperature required for the reduction of the most unstable part of the tungstate layer has decreased to a range where intermediate W(IV) species are already stable on the alumina surface. In MoO_3/Al_2O_3 catalysts, which may be considered a structure analogon as far as their oxidized state (i.e., the initial state) is concerned (*39*), the stabilizing influence of the support is smaller than that in the WO_3/Al_2O_3 system, and Mo(V) and Mo(IV) are the reduction products observed at temperatures as low as 773 K (*38, 40*).

CONCLUSIONS

The reduction of WO_3 and $Al_2(WO_4)_3$, which begins in the same temperature region (~673 K), takes a different course at high temperatures. WO_3 is reduced via W(V), W(IV), and a form that may be W(IV) paired in a particular crystallographic structure to W(0). While the reduction of WO_3 is complete at 973 K, $Al_2(WO_4)_3$ yields a complex system at this temperature in which Al^{3+} is not reduced while tungsten is mainly present as W(VI), W(IV), and W(0).

In WO_3/Al_2O_3 catalysts, the Al_2O_3 support exerts a strong stabilizing effect on W(VI) and W(IV). For catalysts of low WO_3 content, which are reduced at temperatures >973 K, W metal is the only reduction product observed after a 2-h H_2 treat-

ment. When the WO_3 content approaches the monolayer capacity of the Al_2O_3 the reduction proceeds at temperatures $\leq$973 K, and W(IV) is found in addition to W(0). The results confirm the monolayer character of the WO_3/Al_2O_3 system. Similar to chromium but at variance with several other metals zero valent tungsten on Al_2O_3 exhibits a negative XPS binding energy shift relative to the bulk metal.

ACKNOWLEDGMENTS

XRD of reduced aluminium tungstate and electron microprobe analysis of catalysts were performed by Dr. P. Kraak and Dr. P. E. Nau (VEB Leuna-Werke, Leuna, GDR), which is gratefully acknowledged.

REFERENCES

1. Mol, J. C., and Moulijn, J. A., "Advances in Catalysis" (D. D. Eley, P. W. Selwood, and P. B. Weisz, Eds.), Vol. 24, p. 131. Academic Press, New York, 1975.
2. Hérisson, J. L., and Chauvin, Y., *Macromol. Chem.* **141,** 161 (1970).
3. Rappé, A. K., and Goddard, W. A., III, *J. Amer. Chem. Soc.* **104,** 448 (1982).
4. Thomas, R., Moulijn, J. A., de Beer, V. J. H., and Medema, J., *J. Mol. Catal.* **8,** 161 (1980).
5. Thomas, R., and Moulijn, J. A., *J. Mol. Catal.* **15,** 157 (1982).
6. Kadushin, A. A., Aliev, R. K., Krylov, O. V., Andreyev, A. A., Edreyeva-Kardshieva, R. M., and Shopov, D. M., *Kinet. Catal.* **23,** 276 (1982).
7. Vaghi, A., Castellan, A., Bart, J. C. J., Giordano, N., and Ragaini, V., *J. Catal.* **42,** 381 (1976).
8. Van Roosmalen, A. A., and Mol, J. C., *J. Catal.* **78,** 17 (1982).
9. Iwasawa, Y., Ogasawara, S., and Soma, M., *Chem. Lett.*, 1039 (1978).
10. Engelhardt, J., Goldwasser, J., and Hall, W. K., *J. Catal.* **76,** 48 (1982).
11. Goldwasser, J., Engelhardt, J., and Hall, W. K., *J. Catal.* **70,** 275 (1981).
12. Salvati, L., Jr., Makovsky, L. E., Stencel, J. M., Brown, F. R., and Hercules, D. M., *J. Phys. Chem.* **85,** 3700 (1981).
13. Thomas, R., van Oers, E. M., de Beer, V. H. J., Medema, J., and Moulijn, J. A., *J. Catal.* **76,** 241 (1982).
14. Andreini, A. A., and Mol, J. C., *J. Colloid Interface Sci.* **84,** 57 (1981).
15. Thomas, R., Moulijn, J. A., and Kerkhof, F. P. J. M., *Recl. Trav. Chim. Pays-Bas* **96,** M134 (1977).
16. Biloen, P., and Pott, G. T., *J. Catal.* **30,** 169 (1973).
17. Chan, S. S., Wachs, I. E., Murrell, L. L., and Dispenziere, N. C., Jr., *J. Catal.* **92,** 1 (1985).
18. Wachs, I. E., and Murrell, L. L., *J. Catal.* **100,** 500 (1986).
19. Chan, S. S., Wachs, I. E., and Murrell, L. L., *J. Catal.* **90,** 150 (1984).
20. Ianibello, A., Marengo, S., Titarelli, P., Morelli, G., and Zecchina, A., *J. Chem. Soc. Faraday Trans. I* **80,** 2209 (1984).
21. Soled, S., Murrell, L. L., Wachs, I. E., and McVicker, G. B., *Prepr. Symp. Div. Petrol. Chem.* **28,** 1310 (1983); Wachs, I. E., Chersich, C. C., and Hardenbergh, J. H., *Appl. Catal.* **13,** 335 (1985).
22. Grünert, W., Shpiro, E. S., Feldhaus, R., Anders, K., Antoshin, G. V., and Minachev, Kh. M., *J. Electron Spectrosc. Relat. Phenom.* **40,** 187 (1986).
23. Scofield, J. H., *J. Electron Spectrosc. Relat. Phenom.* **8,** 129 (1976).
24. Madey, T. E., Yates, J. T., Jr., and Erickson, N. E., *Surf. Sci.* **43,** 526 (1974).
25. Ng, K. T., and Hercules, D. M., *J. Phys. Chem.* **80,** 2094 (1976).
26. Salje, E., Carley, A. F., and Roberts, M. W., *J. Solid State Chem.* **29,** 237 (1979).
27. Haber, J., Stoch, J., and Ungier, L., *J. Solid State Chem.* **19,** 113 (1976).
28. Minachev, Kh. M., Antoshin, G. V., and Shpiro, E. S., "Fotoelektronnaya spektroskopiya i eyo primeneniye v katalize (Photoelectron Spectroscopy and its Application in Catalysis), Nauka, Moscow, 1981.
29. Khan, A. Z., Antoshin, G. V., Shpiro, E. S., Erivanskaya, L. A., Lunin, V. V., and Minachev, Kh. M., *React. Kinet. Catal. Lett.* **23,** 221, 227 (1983).
30. Khan, A. Z., Shpiro, E. S., Antoshin, G. V., Erivanskaya, L. A., Lunin, V. V., and Minachev, Kh. M., *Surface (Russ.)* **1,** 68 (1985).
31. Myers, B. L., and Mieville, R. L., *Appl. Catal.* **14,** 297 (1985).
32. Mörke, W., and Grünert, W., to be published.
33. Benson, J. E., Kohn, H. W., and Boudart, M. J., *J. Catal.* **5,** 357 (1966).
34. Huizinga, T., vant Blik, H. F., Vis, J. C., and Prins, R., *Surf. Sci.* **135,** 580 (1983).
35. Bastl, Z., Přibyl, O., and Mikušik, P., *Czech. J. Phys. B* **34,** 981 (1984); Bastl, Z., and Mikušik, P., *Czech. J. Phys. B* **34,** 989 (1984).
36. Shpiro, E. S., Dyusenbina, B. B., Antoshin, G. V., Tkachenko, O. P., and Minachev, Kh. M., *Kinet. Catal.* **25,** 1505 (1984); Shpiro, E. S., Dyusenbina, B. B., Tkachenko, O. P., Antoshin, G. V., and Minachev, Kh. M., *Kinet. Catal.* **27,** 638 (1986).

37. Grünert, W., Shpiro, E. S., Feldhaus, R., Anders, K., Antoshin, G. V., and Minachev, Kh. M., *J. Catal.* **100,** 138 (1986).
38. Grünert, W., and Shpiro, E. S., unpublished results.
39. Cirillo, A. C., Jr., Dereppe, J. M., and Hall, W. K., *J. Catal.* **61,** 170 (1980); Liu, H. C., and Weller, S. W., *J. Catal.* **66,** 65 (1980).
40. Patterson, T. A., Carver, J. C., Leyden, D. E., and Hercules, D. M., J. Phys. Chem. **80,** 1700 (1976); Nikishenko, S. B., Slinkin, A. A., Shpiro, E. S., Antoshin, G. V., and Minachev, Kh. M., *Kinet. Catal.* **20,** 524 (1979); Zingg, D. S., Makovsky, L. E., Tischer, R. E., Brown, F. R., and Hercules, D. M., *J. Phys. Chem.* **84,** 2898 (1980).